Optical Second-Harmonic Generation in Reflection from Media with Inversion Symmetry*

N. BLOEMBERGEN, R. K. CHANG,† S. S. JHA, AND C. H. LEE‡
Division of Engineering and Applied Physics, Harvard University, Cambridge, Massachusetts
(Received 6 May 1968)

The radiation at the boundary of an isotropic or cubic medium by a polarization at 2ω, the amplitude of which is proportional to the product of the incident laser field at ω and a spatial derivative of this field, is examined theoretically. A complete expression for the intensity and polarization of the reflected harmonic radiation as a function of the angle of incidence and state of polarization of the incident laser beam is derived. The angular dependences are in good agreement with observations on Si, Ge, and Ag. Some additional experimental results, not previously reported, are described. The magnitude of the nonlinearity due to bound electrons in these cubic materials is related to the square of the linear susceptibility, and agrees qualitatively with observations in Si, Ge, and alkali halides. This nonlinearity has the same order of magnitude as that caused by conduction electrons in metals, which has been extensively discussed in the literature. The influence of absorbed surface layers is considered.

I. INTRODUCTION

THE second-harmonic (SH) generation of light in a medium with inversion symmetry was first observed by Terhune and co-workers[1] in calcite. A detailed theoretical discussion of this quadrupolar type of interaction was given by Pershan[2] and by Adler.[3] They also considered magnetic dipole terms. For the special case of free electrons, these had also been discussed by Bloembergen[4] and by Kronig.[5]

A general theory for the generation of harmonic light in the reflected direction at the boundary of a nonlinear medium had been developed previously.[6] Reflected harmonics from crystals without inversion symmetry had been extensively studied,[7] but the reflected harmonic intensity arising from quadrupolar type terms is, of course, much weaker. They were first observed by Brown and co-workers[8] in silver. Jha[9] showed that the nonlinearity of the conduction electrons arises from a "surface-type" quadrupolar term in addition to the volume term with magnetic dipole character from the Lorentz force considered previously. It was clear from Brown's data that the surface-type term is dominant. It is caused by the discontinuity of the normal component of the electric field strength at the surface. The normal derivative of the normal component of the field behaves as a δ function. In this paper this quasi-discontinuity will be analyzed more carefully.

Bloembergen *et al.*[10] pointed out that similar quadrupole-type surface terms should also occur in insulators. The optical nonlinearity originates in this case from bound electrons, i.e., valence electrons in semiconductors or ion core electrons in ionic crystals. The harmonic generation was soon found experimentally in silicon and germanium[10] and it was shown that in silver, gold, and their alloys the contributions of valence, or d-band electrons, and conduction electrons are of equal importance.[11] More recently, Wang and Duminski[12] have demonstrated the existence of the same effect, but smaller in magnitude, in alkali halides and other ionic crystals with very sensitive equipment.

In this paper we present first the experimental method and apparatus used to detect the SH generation (SHG) from some semiconductors and metals. Experimental results on the polarization and directional dependence of the SHG generation in silicon and germanium are presented in Sec. III. Some previously published results are also tabulated.

A theoretical expression for the magnitude of the quadrupolar-type harmonic polarization on the basis of localized electronic orbitals is derived in Sec. IV. This treatment leads to a simple relationship between this nonlinearity and the bulk linear susceptibility. Next, the directional and polarization properties of the harmonic-reflected radiation from isotropic and cubic crystals is reviewed. This discussion is more complete than in previous publications and integrates the various contributions. Particular attention is paid to the limiting behavior and quasidiscontinuity at the surface.

In Sec. V, the theory is compared with the experimental results of the present and previously published work. The influence of adsorbed surface layers on SH signals is discussed.

* Research supported by the U. S. Office of Naval Research, the Signal Corps of the U. S. Army, and the U. S. Air Force.
† Present address: Dunham Laboratory, Yale University, New Haven, Conn.
‡ Present address, IBM Research Laboratory, San Jose, Calif.
[1] R. W. Terhune, P. D. Maker, and C. M. Savage, Phys. Rev. Letters **8**, 404 (1962).
[2] P. S. Pershan, Phys. Rev. **130**, 919 (1963).
[3] E. Adler, Phys. Rev. **134**, A728 (1964).
[4] N. Bloembergen, Proc. IEEE **51**, 124 (1963).
[5] R. Kronig and J. I. Boukema, Koninkl. Ned. Akad. Wetanschap. Proc. Ser. B **66**, 8 (1963).
[6] N. Bloembergen and P. S. Pershan, Phys. Rev. **128**, 606 (1962).
[7] N. Bloembergen, Opt. Acta **13**, 311 (1966), and references therein.
[8] F. Brown, R. E. Parks, and A. M. Sleeper, Phys. Rev. Letters **14**, 1029 (1965).
[9] S. S. Jha, Phys. Rev. Letters **15**, 412 (1965); Phys. Rev. **140**, A2020 (1965).
[10] N. Bloembergen and R. K. Chang, *Proceedings of the Physics of Quantum Electronics Conference*, edited by P. L. Kelley, B. Lax, and P. E. Tannenwald (McGraw-Hill Book Co., New York, 1966), p. 80.
[11] N. Bloembergen, R. K. Chang, and C. H. Lee, Phys. Rev. Letters **16**, 986 (1966).
[12] C. C. Wang and A. N. Duminski, Phys. Rev. Letters **20**, 668 (1968).

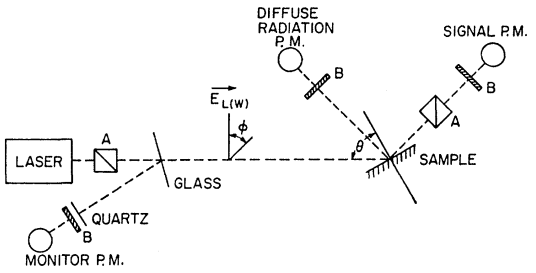

FIG. 1. Experimental method to detect SH reflected light from media with inversion symmetry. (A) Glen-Thomson polarization analyzers; (B) $CuSO_4$ solution filters.

II. EXPERIMENTAL TECHNIQUE

A. Apparatus and Experimental Method

The experimental arrangement is shown in Fig. 1. The Q-switched laser emission can be that of ruby, Nd glass, or stimulated Raman scattering from organic liquids. Both the laser polarization-direction ϕ and the angle of incidence θ on the sample can be varied. The polarization of the SH radiation can be analyzed. The signal photomultiplier is always aligned to be in the direction of the reflected ray, while the photomultiplier used to detect diffused radiation, which might occur from thermal heating, is aligned to face the sample at some arbitrary angle. Surface destruction and concurrent thermal radiation are the major limitations to the amount of laser power density which can be incident on the sample. The thermal radiation was found to have a laser power density (W/cm^2) threshold, whereas the SH intensity varies as $(W/cm^2)\times(cm^2)$. Therefore, it is more advantageous to expand the laser beam cross section than to attenuate the laser intensity by filters. The typical area we used was 2–3 cm^2. Whenever the diffuse radiation phototube registers a photocurrent during the laser pulse, the corresponding signal data of this pulse are discarded.

The laser beam is monitored in the usual way by detecting the amount of SHG from a Z-cut quartz platelet. The reflection from the glass beam splitter is essentially independent of the laser polarization, because the angle of incidence on this glass slide is less than 10°.

The SH signal must pass the usual tests: (a) It must be monochromatic and occur at the harmonic frequency of the fundamental. (b) It must be time-correlated with the monitor signal ($\sim$20 nsec), and not time-correlated with the diffuse radiation signal, if any. (c) It must be collimated along the reflection direction. In order to obtain the absolute intensity of the observed SH signal from the sample, a relative measurement was made between the SHG from a (110)-face GaAs mirror and that from the samples, as the former had been calibrated absolutely.[13] Fundamental beams at different frequencies were obtained by using a ruby laser, a Nd-glass laser, and the stimulated Raman effect from a ruby laser in cyclohexane and nitrobenzene.

[13] R. K. Chang, J. Ducuing, and N. Bloembergen, Phys. Rev. Letters **15**, 415 (1965).

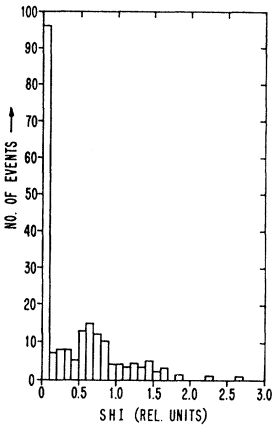

FIG. 2. The distribution in the number of photoelectrons caused by the SH signal from a silver mirror when the fundamental electric field is polarized normal to the plane of incidence.

During a laser pulse containing about 10^{18} incident quanta, about 40–2000 reflected harmonic quanta are typically emitted from these media which possess a bulk center of inversion. These give rise to 1–50 photoelectrons at the photocathode. Photon-counting techniques must be employed to measure the weak signals accurately. Typical SH intensity data obtained for two different fundamental polarizations on a Ag sample are shown in Figs. 2 and 3, where the number of events versus photocurrent height are plotted. The average height of one photoelectron, which can be determined from the dark current of the photomultiplier, is 0.7 units.

The distribution of Fig. 2 is fitted with respect to a Poisson distribution

$$P_n=(\bar{n})^n e^{-\bar{n}}/n!\,,$$

where P_n is the probability of detecting n photons and $\bar{n}$ is the average number of photons. For the data shown in Fig. 2, one finds that

$$\bar{n}=P_1/P_0=75/103=0.73\,,$$

which is consistent with

$$\bar{n}=2P_2/P_1=2\times25/75=0.67.$$

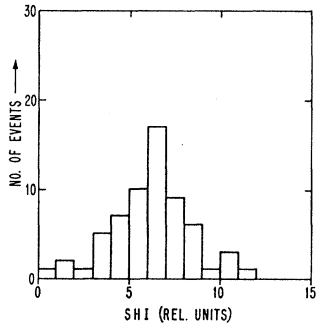

FIG. 3. The distribution in the number of photoelectrons caused by the SH signal from a Ag mirror when the fundamental electric field is polarized in the plane of incidence.

TABLE I. The ratio M of the SH reflected intensity when the incident laser beam, incident at 45°, is polarized perpendicular and parallel to the plane of incidence, respectively.

	Harmonic-photon energy (eV)	M expt.	M core linear	M core linear and nonlinear
Ag	3.58	0.066±0.013	0.068	0.084
Ag	2.87	0.066±0.013	0.042	0.060
Au	3.58	0.083±0.016	0.038	

The distribution of Fig. 3 is fitted with respect to a Gaussian with $\bar{n} \approx 10$. The ratio M between SH intensity when the laser is polarized perpendicular and parallel to the plane of incidence is tabulated in Table I. In the above example shown in Figs. 2 and 3, the ratio is 0.07, with a "confidence level" such that if the measurements are repeated this value for the ratio will be within 20%.

The data in Fig. 3 represent one of the largest signals encountered in this kind of work. Recently, Wang and Duminski[12] have refined the statistical photon counting to signals significantly smaller than those corresponding to the data in Fig. 2. The largest signals occur in media with high linear optical susceptibilities. The signals in alkali halides, found by Wang and Duminski, are significantly smaller than those in the metals and semiconductors studied by us.

B. Special Techniques

Since the signals cannot be increased by increasing the laser flux density because of the limits imposed by thermal radiation and material damage, a method of multiple reflection has been attempted to enhance the signal-to-noise ratio. Two parallel Ag mirrors are contained in a dry box in which the pressure of the air can be varied. In this manner, the phase relationship between fundamental and SH waves can be adjusted so that constructive interference occurs on successive reflections. For a total of three reflections, it has been possible to increase the SH signal by a factor of 6, in agreement with theoretical calculations. Because of reflection losses occurring in both the fundamental and SH beams, it will be difficult to improve the signal to noise by more than an order of magnitude in metals. For semiconductors and insulators this method cannot be used effectively.

When our experiments were started, there was a widespread belief that such harmonic signals would arise only from conduction electrons. It was suggested that the laser beam first created a conduction-electron plasma in our semiconductor samples, and that the nonlinear signal created by this plasma was observed. This has been disproved in the following two ways. First, the reflectivity of the Si and Ge samples was monitored with a continous beam at 6328 Å from a He-Ne laser. No observable change in the reflectivity, $\Delta R/R$, occurred during the giant Q-switched laser pulse which generated the SH intensity. In fact, with a Nd laser pulse, a power level of 15 times over the usual operating power level for detecting SHG from Ge is required to detect a $\Delta R/R \approx 3\%$. Therefore, the induced conduction-electron density produces a negligible change in the linear dielectric constant at the power level used in our experiment. This puts an upper limit on the concentration of conduction electrons, and this concentration could at most produce 1% of the observed signal. In the second place, the signals in Si and Ge were found to be strictly proportional to the square of the laser intensity. If conduction electrons must be first created and then their nonlinear properties taken, the SHG would be proportional to the fourth power of the fundamental intensity.

C. Sample Preparation

Measurements of SHG have been made on Ag, Au, Cu, Al, Ag-Au alloys, Si, and Ge. All the metallic samples were evaporated onto a clean microscope slide substrate in vacuum of 10^{-6}–10^{-7} Torr. The Ag-Au alloys were made by simultaneously controlled evaporation of Ag and Au. The percentage of composition and homogeneity of the samples were analyzed by a nondestructive quantitative electron-probe microanalysis through a customer service of the Advance Metals Research Corporation. The precision on the relative composition and homogeneity was ±3% for all the 19 samples. The thickness of all the samples was about a few microns. The metallic samples were continually flushed by N_2 gas when SHG data were being taken, or stored in a N_2-filled box. Within a few weeks, no change in the SHG data could be noticed as a result of possible tarnishing.

Both Si and Ge were thin slabs of single crystals. Their typical dimensions were $2.5 \times 2 \times 0.2$ cm^3. One face of the crystal was polished by a sequence of 1-, 0.3-, and 0.05-μ Linde abrasives. The polished surface was then mildly etched. The crystallographic orientations of the surface were [111], [100], and [110], respectively. The signals for different cuts were essentially the same.

III. EXPERIMENTAL RESULTS

A. Polarization and Angular Dependence

Originally, the striking directional properties of the SHG from Ag, observed by Brown and co-workers,[14] were considered as proof that the nonlinearities arose from free electrons. The directional properties of the SH generated from Si and Ge is, however, quite similar to that emitted from metals. In Fig. 4 the SH intensity polarized in the plane of reflection, generated by a laser beam with an angle of incidence $\theta = 45°$, is plotted as a function of the angle ϕ between the electric field vector of the laser and the plane of incidence. The curves for both Ag and Si are rather well described by a dominant

[14] F. Brown and R. E. Parks, Phys. Rev. Letters **16**, 507 (1966); see also Ref. 8.

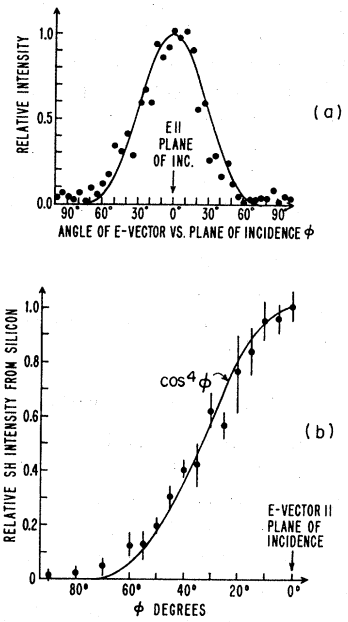

FIG. 4. Variation of the SH intensity as a function of angle ϕ between the fundamental electric vector and the plane of incidence. The angle of incidence is 45°. (a) data for Ag (Ref. 8); (b) data for Ge (Ref. 10). The solid line representing a $\cos^4\phi$ dependence is drawn for comparison.

contribution proportional to $\cos^4\phi$. The SH intensity for $\phi=\frac{1}{2}\pi$ does not, however, completely vanish. In the first column of Table I, the experimental ratio M for the intensities at $\phi=90°$ and $\phi=0°$ is listed for a number of materials.

The dependence of the SH intensity as a function of the angle of incidence θ, for $\phi=0°$, is shown in Fig. 5. Again the behavior for Si and Ag is very similar. It is evident from the theory, as will be discussed more fully in Sec. IV, that this general behavior may be expected from all materials that have a very high linear dielectric constant. It has little to do with the question whether the electrons are free or bound. The same angular dependence on θ for Ag has been reported by Sonnenberg and Heffner.[15]

B. Magnitude and Dispersion of the Nonlinearity

Since the effect in media with inversion symmetry is a quadrupole effect, one may expect that the SH signal from Ge will be smaller by a factor $|ka|^2$ in order of magnitude from that in GaAs. The latter crystal has a similar structure, but since it lacks a center of inversion an electric dipole effect is operative in it. The magnitude of the wave vector k inside the medium is essentially equal to the inverse of the absorption depth of the SH light; a is a typical atomic dimension. The effect in Si and Ge is indeed about three orders of magnitude smaller than in the corresponding III-V compounds. The effect in Ge has the same order of magnitude as

[15] H. Sonnenberg and H. Heffner, J. Opt. Soc. Am. 58, 209 (1968).

TABLE II. The magnitude of the SH intensity, polarized in the plane of incidence, created by a fundamental beam also polarized in the plane of incidence. The angle of incidence is 45°. The tabulated quantity is $10^{18}|E_{2\|}{}^R(\theta=45°,\phi=0°)|^2/|E_1(\omega)|^4$, with the fields expressed in statvolts.

Harmonic photon energy (eV)	Si	Ge	Ag	Au
2.34	0.3	···	1.7	···
2.87	0.65	1.5	9.0	2.7
3.24	2.0	···	6.5	2.0
3.58	2.5	2.0	6.0	1.0

that in Au. In Table II, we list the SH intensity, divided by the square of the indirect laser intensity. Both beams are polarized in the plane of incidence and the angle of incidence $\theta=45°$. The data are given for four different frequencies. The harmonic dispersion curve in silicon is plotted in Fig. 6, where the linear susceptibility has been given for comparison. Both quantities increase, when interband resonances are approached. Dispersion curves for Ag and Au and SHG in Ag-Au alloys have been published elsewhere.[11] The relative magnitude of the effect in Si, Ge, Ag, and Au, shown in Table II, is quite comparable to the data published recently by Wang and Duminski, who used a somewhat different geometry at the ruby wavelength. The SH intensity is strongly influenced by the linear dispersion through the

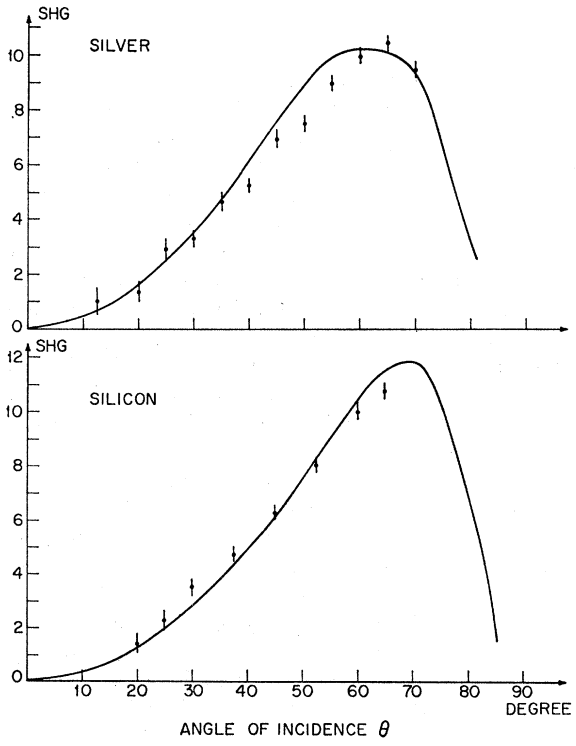

FIG. 5. The variation of the SH intensity in Si and Ag as a function of the angle of incidence. The fundamental electric field vector lies in the plane of incidence, $\phi=0°$. The drawn curves are derived from the theory, discussed in Secs. IV and V.

Fresnel factors. In addition, there is an intrinsic dispersion in the nonlinearity. The data show again that the interband contribution of the valence electrons in Si and Ge is quite comparable to the nonlinearity in Au and Ag. In Au and Ag, the nonlinear interband contributions from the d electrons is comparable to that of the conduction electrons, since the d electrons also contribute significantly to the linear dielectric constant in these metals. This has been discussed in several papers.[16,17] In Secs. IV and V the theory for the nonlinear contribution from bound electrons will be analyzed more precisely.

IV. THEORY OF SHG FROM MEDIA WITH INVERSION SYMMETRY

General expressions for the calculation of nonlinear source terms, including the contribution of both conduction and valence electrons and of all multipole moments, may be derived from standard time-dependent perturbation theory. Cheng and Miller[18] have given complete expressions for the second-order nonlinear sources for Bloch electron wave functions in crystals. For a practical evaluation of the nonlinearity, it is advantageous to use localized electron orbitals and expand the interaction Hamiltonian between the radiation field and the electrons as well as the nonlinear current density in a multipole series.

The interaction Hamiltonian may be written in the form

$$\mathcal{H}_1=-\mathbf{P}\cdot\mathbf{E}(\mathbf{R},t)-\mathbf{M}\cdot\mathbf{H}(\mathbf{R},t)-\mathbf{Q}:\nabla_{\mathbf{R}}\mathbf{E}(\mathbf{R},t), \quad (1)$$

with

$$\mathbf{P}=-e\mathbf{x},$$

$$\mathbf{M}=-\frac{e}{2mc}(\mathbf{x}\times\mathbf{p})=-\frac{e}{2mc}\mathbf{L},$$

$$\mathbf{Q}=-\tfrac{1}{2}e\mathbf{x}\mathbf{x},$$

where $\mathbf{R}$ is the origin of the unit cell under consideration and $\mathbf{x}$ is the relative displacement operator.

The diamagnetic term $e^2/8mc^2(\mathbf{H}\times\mathbf{x})^2$, which is proportional to $(\nabla_{\mathbf{R}}\mathbf{A})^2$, has been omitted. In the same approximation, the total current density due to all electrons becomes

$$\mathbf{J}=N\left[\frac{\partial}{\partial t}\langle\mathbf{P}\rangle_{\text{cell}}+c\nabla_{\mathbf{R}}\times\langle\mathbf{M}\rangle_{\text{cell}}-\frac{\partial}{\partial t}\nabla_{\mathbf{R}}\cdot\langle\mathbf{Q}\rangle_{\text{cell}}\right], \quad (2)$$

where N is the number of unit cells per unit volume and $\langle\ \rangle_{\text{cell}}$ implies sum of the expectation values for all the electrons in the cell.

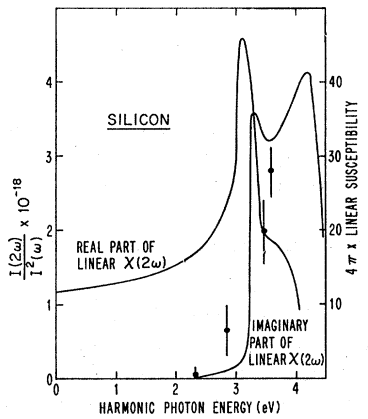

FIG. 6. The frequency dependence for the reflected SH intensity from Si, for $\theta=45°$, $\phi=0°$. The dispersion of the linear susceptibility is shown for comparison.

By expanding

$$\mathbf{E}(R,t)=\sum_{\omega}\mathbf{E}(R,\omega)e^{-i\omega t},$$

$$\mathbf{H}(R,t)=\sum_{\omega}\mathbf{H}(R,\omega)e^{-i\omega t},$$

so that

$$\mathcal{H}_1(t)=\sum_{\omega}\mathcal{H}_1(\omega)e^{-i\omega t},$$

and using well-known time-dependent perturbation theory, it is straightforward to find the expectation value of a time-independent operator G in the perturbed state. If the unperturbed system in the ground state is $|0\rangle$, one obtains

$$\langle G\rangle_{\text{pert}}=G_0+\sum_{\omega}G_1(\omega)e^{-i\omega t}+\sum_{\omega_1+\omega_2}G_2(\omega_1+\omega_2)e^{-i(\omega_1+\omega_2)t}+\cdots, \quad (3)$$

where

$$G_0=\langle 0|G|0\rangle$$

$$G_1(\omega)=-\sum_m\left[\frac{\langle 0|\mathcal{H}_1(\omega)|m\rangle\langle m|G|0\rangle}{(E_m-E_0+\hbar\omega)}+\frac{\langle 0|G|m\rangle\langle m|\mathcal{H}_1(\omega)|0\rangle}{(E_m-E_0-\hbar\omega)}\right],$$

$$G_2(\omega_1+\omega_2)=\sum_m\sum_n\left[\frac{\langle 0|\mathcal{H}_1(\omega_1)|m\rangle\langle m|\mathcal{H}_1(\omega_2)|n\rangle\langle n|G|0\rangle}{(E_m-E_0+\hbar\omega_1)(E_n-E_0+\hbar\omega_{12})}+\frac{\langle 0|\mathcal{H}_1(\omega_2)|m\rangle\langle m|G|n\rangle\langle n|\mathcal{H}_1(\omega_1)|0\rangle}{(E_m-E_0+\hbar\omega_2)(E_n-E_0-\hbar\omega_1)}+\frac{\langle 0|G|m\rangle\langle m|\mathcal{H}_1(\omega_1)|n\rangle\langle n|\mathcal{H}_1(\omega_2)|0\rangle}{(E_m-E_0-\hbar\omega_{12})(E_n-E_0-\hbar\omega_2)}\right]$$

$$+(\text{terms with }\omega_1\rightleftarrows\omega_2,\text{ if }\omega_1\neq\omega_2), \quad (4)$$

[16] S. S. Jha and C. S. Warke, Phys. Rev. **153**, 751 (1967); **162**, 854(E) (1967).
[17] K. C. Rustagi, Nuovo Cimento **53B**, 346 (1968).
[18] H. Cheng and P. B. Miller, Phys. Rev. **134**, A683 (1964); see also Ref. 17.

and where

$$\omega_{12}=\omega_1+\omega_2$$
$$\mathcal{H}_0|m\rangle=E_m|m\rangle.$$

The second-order nonlinear current density may be calculated from Eqs. (2)–(4). The various combinations of terms have been discussed by Adler.[3]

A. Quadrupolar Contribution from Localized Orbitals

We are interested in estimating the lowest-order nonlinear contribution from bound electrons in nonmagnetic crystals with inversion symmetry. In this case, one collects the terms in Eq. (2) in the nonlinear current which are proportional to the spatial derivative of a quadratic expression in the field components. In the expressions for G_2 one uses the quadrupole operator once and the electric dipole moment operator twice. With $\omega_1=\omega_2=\omega$, one finds for the SH source term,

$$P^{\mathrm{NL},Q}{}_i(2\omega)=J^{\mathrm{NL},Q}{}_i(2\omega)/-2i\omega$$
$$=N(\Gamma_{jl,ki}-\Gamma_{ij,kl})E_j(\omega)\nabla_k E_l(\omega). \quad (5)$$

In the limit of low frequencies, in which case the dispersion of the nonlinearity may be ignored, the expressions for Γ become symmetric in both the first and the last pair of indices and simplify to

$$\Gamma_{ij,kl}=\tfrac{1}{2}e^3\sum_m{}'\sum_n{}'\frac{1}{(E_m-E_0)(E_n-E_0)}$$
$$\times[\langle 0|\bar{x}_i|m\rangle\langle m|(x_kx_l)_{\mathrm{o.d.}}|n\rangle\langle n|\bar{x}_j|0\rangle$$
$$+\langle 0|\bar{x}_i|m\rangle\langle m|\bar{x}_j|n\rangle\langle n|(x_kx_l)_{\mathrm{o.d.}}|0\rangle$$
$$+\langle 0|(x_kx_l)_{\mathrm{o.d.}}|m\rangle\langle m|\bar{x}_i|n\rangle\langle n|\bar{x}_j|0\rangle+(j\rightleftarrows i)], \quad (6)$$

with

$$\bar{x}_i=x_i-\langle 0|x_i|0\rangle=x_i,$$
$$(x_kx_l)_{\mathrm{o.d.}}=x_kx_l-\langle 0|x_kx_l|0\rangle,$$

and

$$\Gamma_{ij,kl}=\Gamma_{ji,kl}=\Gamma_{ij,lk}.$$

The structure of Eqs. (5) and (6) is consistent with the general form of the quadrupole volume source term discussed by Pershan.[2] For a cubic or isotropic material, the expression simplifies to

$$P^{\mathrm{NL},Q}{}_i(2\omega)=N(\Gamma_{xy,xy}-\Gamma_{xx,yy})(E_i\nabla_jE_j-E_j\nabla_iE_j). \quad (7)$$

If we can replace all energy denominators in Eq. (6) by some average energy denominator $\hbar\omega_0$ (closure approximation), we obtain

$$\Gamma_{ij,kl}\approx\frac{3e^3}{\hbar^2\omega_0{}^2}\sum_{\mathrm{el}}[\langle 0|x_ix_jx_kx_l|0\rangle$$
$$-\langle 0|x_ix_j|0\rangle\langle 0|x_kx_l|0\rangle], \quad (8)$$

where we have to sum over all the electrons in the cell.

For a cubic or isotropic material, Eqs. (7) and (8) reduce to

$$N(\Gamma_{xy,xy}-\Gamma_{xx,yy})=(3\mathfrak{N}e^3/\hbar^2\omega_0{}^2)(\langle 0|x^2|0\rangle)^2,$$

where $\mathfrak{N}$ is the density of valence electrons. Since, in the same approximation, the linear susceptibility is given by

$$\chi^L{}_{\omega\to 0}(\omega)=(2\mathfrak{N}e^2/\hbar\omega_0)\langle 0|x^2|0\rangle, \quad (9)$$

we find that the nonlinear SH source term from bound electrons in cubic or isotropic media with inversion symmetry may be written, in the low-frequency limit, as

$$P^{\mathrm{NL},Q}{}_i\approx(3/4\mathfrak{N}e)(\chi^L)^2(E_i\nabla_jE_j-E_j\nabla_iE_j). \quad (10)$$

B. Contribution of Conduction Electrons

In this case, the low-frequency approximation discussed above is, of course, inapplicable. Furthermore the magnetic-dipole contribution cannot be neglected. Although the nonlinearity of an electron gas has been discussed extensively in the literature, especially by Jha and co-workers,[9,17] we shall give here a very brief derivation of the nonlinear source terms in a form suitable for comparison with the bound-electron contribution and with experiment.

In the absence of interband transitions, it is well known that the response of the conduction electrons to external electromagnetic fields may be calculated classically. If we treat the electrons in the conduction band with average effective mass m^* as a gas, in presence of the self-consistent fields $\mathbf{E}(\mathbf{r},t)$ and $\mathbf{H}(\mathbf{r},t)$, the hydrodynamic equation of motion for the average velocity $\mathbf{V}$ is given by

$$\partial\mathbf{V}/\partial t+\mathbf{V}\cdot\boldsymbol{\nabla}\mathbf{V}=-(e/m^*)(\mathbf{E}+c^{-1}\mathbf{V}\times\mathbf{H}). \quad (11)$$

In addition, we have the Maxwell equation

$$\boldsymbol{\nabla}\cdot\mathbf{E}=-4\pi e(n-n_0) \quad (12)$$

and the continuity equation

$$\partial n/\partial t=-\boldsymbol{\nabla}\cdot(n\mathbf{V}), \quad (13)$$

where n is the number density and $\mathbf{J}=-ne\mathbf{V}$ is the electric current density. In writing Eq. (11) we have ignored a pressure term which one obtains while integrating the Boltzmann equation,[19] assuming that this is balanced by the force due to the surface-barrier potential. By expanding

$$\mathbf{E}=\mathbf{E}(\omega)e^{-i\omega t}+\mathbf{E}(2\omega)e^{-2i\omega t}+\text{c.c.},$$
$$\mathbf{H}=\mathbf{H}(\omega)e^{-i\omega t}+\mathbf{H}(2\omega)e^{-2i\omega t}+\text{c.c.},$$
$$\mathbf{V}=\mathbf{V}_1e^{-i\omega t}+\mathbf{V}_2e^{-2i\omega t}+\text{c.c.},$$
$$n=n_0+n_1e^{-i\omega t}+n_2e^{-2i\omega t}+\cdots,$$

we may solve Eqs. (11) and (12) by successive approximation to find that the nonlinear part of the second-

[19] See, e.g., S. Chandrashekhar, *Plasma Physics* (The University of Chicago Press, Chicago, 1960), p. 5.

order polarization induced in the gas is given by

$$\mathbf{P}_{\text{cond}}^{\text{NL}}(2\omega)=\frac{\mathbf{J}_2^{\text{NL}}(2\omega)}{-2i\omega}=\frac{e}{2i\omega}(n_0\mathbf{V}_2+n_1\mathbf{V}_1)$$
$$=(n_0e^3/4m^{*2}\omega^4)[\mathbf{E}(\omega)\cdot\nabla]\mathbf{E}(\omega)$$
$$+(e/8\pi m^*\omega^2)\mathbf{E}(\omega)\nabla\cdot\mathbf{E}(\omega)$$
$$+(in_0e^3/4m^{*2}c\omega^3)\mathbf{E}(\omega)\times\mathbf{H}(\omega). \quad (14)$$

C. General Form of Source Term in Isotropic Media

Regardless of the detailed mechanism and models for the nonlinearity, the nonlinear polarization in an isotropic centrosymmetric medium may always be written in the vector form

$$\mathbf{P}^{\text{NL}}(2\omega)=(\delta-\beta-2\gamma)(\mathbf{E}(\omega)\cdot\nabla)\mathbf{E}(\omega)$$
$$+\beta\mathbf{E}(\omega)(\nabla\cdot\mathbf{E}(\omega))+\gamma\nabla(\mathbf{E}(\omega)\cdot\mathbf{E}(\omega)). \quad (15)$$

This is equivalent to the form

$$\mathbf{P}^{\text{NL}}(2\omega)=(\delta-\beta)(\mathbf{E}(\omega)\cdot\nabla)\mathbf{E}(\omega)$$
$$+\beta\mathbf{E}(\omega)(\nabla\cdot\mathbf{E}(\omega))+\alpha\mathbf{E}(\omega)\times\mathbf{H}(\omega), \quad (16)$$

with $\alpha=(2i\omega/c)\gamma$.

Comparison of Eqs. (15) and (10) show that for an isotropic (or cubic) insulating medium one has, in the low-frequency limit,

$$\beta=-2\gamma\approx\frac{3}{4\mathfrak{N}e}[\chi^L(\omega)]^2, \quad \delta=0. \quad (17)$$

In this approximation, cubic crystals also behave as isotropic media as far as the quadrupolar SH generation is concerned.

For conducting media we have to add the nonlinear plasma contribution. Comparison of Eqs. (15) and (14) shows that

$$\beta_{\text{pl}}=e/8\pi m^*\omega^2,$$
$$\gamma_{\text{pl}}=\frac{c}{2i\omega}\alpha_{\text{pl}}=\frac{n_0e^3}{8m^{*2}\omega^4}=\beta_{\text{pl}}\left(\frac{\omega_p^2}{4\omega^2}\right), \quad (18)$$
$$\delta_{\text{pl}}=\beta_{\text{pl}}+2\gamma_{\text{pl}},$$

where $\omega_p^2=4\pi n_0e^2/m^*$ is the plasma frequency.

This value of δ_{pl} should not be taken too literally. This term is very sensitive to the hydrodynamic pressure and the surface potential gradient which act normal to the surface. The true value of δ_{pl} is probably much smaller.

D. SH Fields Generated by Nonlinear Quadrupolar Source Terms

Let us assume that a plane wave of frequency ω is incident from the vacuum at an angle θ on the plane boundary of a solid. Let us choose the coordinate system such that the boundary is given by $z=0$, and the plane of incidence is $y=0$, the solid occupying the half-space $z\leqslant 0$. Thus the incident light wave is given by

$$\mathbf{E}_{\text{inc}}=\mathbf{E}_{\text{inc}}^{(0)}\exp[(-i\omega/c)z\cos\theta]$$
$$\times\exp[(-i\omega/c)x\sin\theta]e^{-i\omega t}+\text{c.c.}, \quad (19)$$

with

$$\mathbf{E}_{\text{inc}}^{(0)}=(E_0\cos\theta\cos\phi, E_0\sin\phi, -E_0\sin\theta\cos\phi), \quad (20)$$

where ϕ is the angle between the plane of incidence and the polarization vector of the incident wave.

The solution of Maxwell's equations for the reflected and transmitted waves at the fundamental frequency ω is given by the usual Fresnel formulas. The differential equation for the Fourier component of the electric field vector at the harmonic frequency is given by

$$\nabla\times\nabla\times\mathbf{E}_2-(4\omega^2/c^2)\epsilon(2\omega)\mathbf{E}_2$$
$$=(16\pi\omega^2/c^2)\mathbf{P}^{\text{NL}}(2\omega), \quad (21)$$

where $\mathbf{P}^{\text{NL}}(2\omega)$ has the form given by Eq. (15). We may solve our problem by finding the general solutions of the equations

$$\nabla\times\nabla\times\mathbf{E}_2-(4\omega^2/c^2)\epsilon(2\omega)\mathbf{E}_2$$
$$=(16\pi\omega^2/c^2)\gamma\nabla(\mathbf{E}_1\cdot\mathbf{E}_1), \quad \text{for} \quad z<0 \quad (22)$$

and

$$\nabla\times\nabla\times\mathbf{E}_2-(4\omega^2/c^2)\mathbf{E}_2=0, \quad \text{for} \quad z>0 \quad (23)$$

and using the following boundary conditions at the surface:

$$\text{(i)} \quad E_{2y}(z=0^+)=E_{2y}(z=0^-), \quad (24)$$

$$\text{(ii)} \quad \left(\frac{\partial E_{2x}}{\partial x}\right)_{z=0^-}^{z=0+}=\frac{16\pi\omega^2}{c^2}\lim_{\eta\to 0}\int_{-\eta}^{+\eta}dz\,P^{\text{NL}}{}_z(2\omega)$$
$$\equiv(16\pi\omega^2/c^2)\tfrac{1}{2}\bar{\delta}[\epsilon^2(\omega)-1]E_{1z}{}^2(z=0^-), \quad (25)$$

$$\text{(iii)} \quad \left(-\frac{\partial E_{2y}}{\partial z}\right)_{z=0^-}^{z=0+}=\frac{16\pi\omega^2}{c^2}\lim_{\eta\to 0}\int_{-\eta}^{+\eta}dzP^{\text{NL}}{}_y(2\omega)$$
$$\equiv(16\pi\omega^2/c^2)\bar{\beta}\{\epsilon(\omega)-1\}E_{1y}E_{1z}(z=0^-), \quad (26)$$

$$\text{(iv)} \quad \left(\frac{\partial E_{2z}}{\partial x}-\frac{\partial E_{2x}}{\partial z}\right)_{z=0^-}^{z=0+}=\frac{16\pi\omega^2}{c^2}\lim_{\eta\to 0}\int_{-\eta}^{+\eta}dzP^{\text{NL}}{}_x(2\omega)$$
$$\equiv(16\pi\omega^2/c^2)\bar{\beta}\{\epsilon(\omega)-1\}E_{1x}E_{1z}(z=0^-), \quad (27)$$

which follow directly from Eqs. (15) and (21).

Note that Eqs. (24)–(27) define $\bar{\delta}$ and $\bar{\beta}$ which are observed experimentally and which are same as δ and β, respectively, only if these are constants (including zero) in the thin layer near the surface. If these change abruptly from their bulk values to zero at the surface, $\bar{\beta}\approx\frac{1}{2}\beta$ and $\bar{\delta}\approx\frac{1}{2}\delta$.

It is straightforward to show that the solution inside the solid is given by

$$\mathbf{E}_2=\mathbf{E}_2{}^T\exp(-ik_{2z}{}^Tz)\exp[(-i2\omega/c)x\sin\theta]$$
$$-\frac{4\pi\gamma}{\epsilon(2\omega)}\nabla\left\{\mathbf{E}_1{}^T\cdot\mathbf{E}_1{}^T\exp(-i2k_{1z}{}^Tz)\right.$$
$$\left.\times\exp\left(\frac{-i2\omega}{c}x\sin\theta\right)\right\},\quad \text{for } z<0. \quad (28)$$

Since the nonlinear volume source term is parallel to the direction of propagation in cubic and isotropic media, the transmitted wave does not grow away from the boundary

The solution for the reflected wave is given by

$$\mathbf{E}_2=\mathbf{E}_2{}^R\exp[(i2\omega/c)z\cos\theta]\exp[(-i2\omega/c)x\sin\theta],\quad \text{for } z>0 \quad (29)$$

where

$$K_{1z}{}^T=(\omega/c)[\epsilon(\omega)-\sin^2\theta]^{1/2}, \quad (30)$$
$$K_{2z}{}^T=(2\omega/c)[\epsilon(2\omega)-\sin^2\theta]^{1/2}, \quad (31)$$
$$E_{2z}{}^T=-E_{2x}{}^T(2\omega\sin\theta)/cK_{2z}{}^T, \quad (32)$$
$$E_{2z}{}^R=E_{2x}{}^R\tan\theta. \quad (33)$$

It is understood that for negative or complex $(K_{1z}{}^T)^2$ and $(K_{2z}{}^T)^2$, $K_{1z}{}^T$ and $K_{2z}{}^T$ are to be calculated from Eqs. (30) and (31) in such a way that their real and imaginary parts are always positive.

Using boundary conditions (24)–(27), one may determine the unknown coefficients $\mathbf{E}_2{}^T$ and $\mathbf{E}_2{}^R$. In general, the reflected harmonic wave has components polarized in the plane of incidence ($E_{2\parallel}{}^R$) as well as perpendicular to the plane of incidence ($E_{2\perp}{}^R$). In terms of the incident field amplitude E_0, we obtain

$$|E_{2\perp}{}^R|=(32\pi\omega/c)E_0{}^2\sin\theta\cos^2\theta\sin\phi\cos\phi$$
$$\times\left|\frac{[\epsilon(\omega)-1]\bar{\beta}}{[\epsilon(\omega)]^{1/2}g_0(\omega)g_1(\omega)g_1(2\omega)}\right| \quad (34)$$

and

$$|E_{2\parallel}{}^R|=(32\pi\omega/c)E_0{}^2\sin\theta\cos^2\theta$$
$$\times|\{[\epsilon(2\omega)]^{1/2}\epsilon(\omega)g_0(2\omega)g_0{}^2(\omega)\}^{-1}|$$
$$\times|[-\gamma\epsilon(\omega)[\cos^2\phi+\sin^2\phi\, g_0{}^2(\omega)/g_1{}^2(\omega)]$$
$$-\tfrac{1}{2}\bar{\delta}[\epsilon^2(\omega)-1]\epsilon(2\omega)\cos^2\phi$$
$$+\bar{\beta}[\epsilon(\omega)-1][\epsilon(\omega)-\sin^2\theta]^{1/2}$$
$$\times[\epsilon(2\omega)-\sin^2\theta]^{1/2}\cos^2\phi]|, \quad (35)$$

where

$$g_0(\omega)=[\epsilon(\omega)]^{1/2}\cos\theta+[1-\epsilon^{-1}(\omega)\sin^2\theta]^{1/2},$$
$$g_0(2\omega)=[\epsilon(2\omega)]^{1/2}\cos\theta+[1-\epsilon^{-1}(2\omega)\sin^2\theta]^{1/2},$$
$$g_1(\omega)=\cos\theta+[\epsilon(\omega)-\sin^2\theta]^{1/2},$$
$$g_1(2\omega)=\cos\theta+[\epsilon(2\omega)-\sin^2\theta]^{1/2}.$$

These equations give the SH amplitude and polarization in terms of the incident fundamental amplitude E_0, as a function of the angle of incidence θ and of the direction of the incident polarization ϕ.

The same expressions could have been obtained directly by making use of the nonlinear boundary problem solved by Bloembergen and Pershan.[6,20] Their Eq. (4.12) gives immediately the term proportional to γ, produced by the volume source term. The surface terms can be derived by taking their Eqs. (6.12) and (6.22) for a layer of thickness d, and letting d approach zero in such a manner that the product $P^{\mathrm{NLS}}d$ remains finite.

Equation (34) follows immediately from their Eq. (6.12) if one substitutes for the source term in the y direction, i.e., normal to the plane of incidence

$$P^{\mathrm{NLS}}{}_y d\rightarrow\int_{-\eta}^{+\eta}\beta E_{1y}\frac{\partial E_{1z}}{\partial z}dz=\bar{\beta}E_{1y}E_{1z}{}^0[\epsilon(\omega)-1]. \quad (36)$$

The term proportional to $\bar{\beta}$ in Eq. (35) follows in the same manner from the last term in Eq. (6.22). We reproduce this equation here, in a slightly modified notation, for the sake of convenience:

$$E_{11}{}^R(2\omega)=-8\pi i\omega dc^{-1}$$
$$\times[P^{\mathrm{NL}}{}_z(2\omega)\epsilon_T{}^{1/2}(2\omega)\sin\theta\,\epsilon^{-1}(z)+\cos\theta_T\,P^{\mathrm{NL}}{}_x(2\omega)]$$
$$\times[\epsilon_T{}^{1/2}(2\omega)\cos\theta+\cos\theta_T]^{-1} \quad (37)$$

where $\epsilon_T(2\omega)$ is the bulk dielectric constant.

The term proportional to δ, due to the z component of the nonlinear polarization $P_z=P^{NLS}\cos(\theta_s+\alpha)=\delta E_z(\partial E_z/\partial_z)$, is very sensitive to the details of the limiting procedure. Not only E_z, but also $\epsilon(z)$, varies rapidly within the layer. Physically the nonlinear coefficient δ also varies drastically at the surface.

In a purely formal manner we find from Eq. (37) a contribution proportional to $\frac{1}{3}\delta(\epsilon^3-1)\sin^2\theta$ instead of $\frac{1}{2}\bar{\delta}[\epsilon^2(\omega)-1]\epsilon(2\omega)$ occurring in Eq. (35). Wang and Duminski[12] apparently assumed that both δ and ϵ are constant within the surface layer and find $\delta\sin^2\theta[\epsilon(\omega)-1]$ instead.

For an insulator, Eq. (17) predicts that δ vanishes in the low-frequency approximation so that the term is probably quite small in any case. Equation (17) also suggests that the nonlinearity is proportional to $[\epsilon(\omega)-1]^2$, provided that we consider the number density $\mathfrak{N}$ as a constant in the surface layer. One could calculate $\bar{\delta}$ and $\bar{\beta}$ on the premise that this relationship between linear and nonlinear coefficients continues to hold on a microscopic scale within the surface layer. Such assumptions are not realistic, but they provide an estimate for the uncertainties involved.

The only correct way to find δ and β is to calculate the actual potential at the boundary, use the appropriate

[20] In Eq. (4.12) of Ref. 6 one must take $\alpha=0$ for the angle for the geometry under consideration. Instead of $\epsilon_s{}^{1/2}$ one should read $\epsilon_R{}^{1/2}$.

wave functions for surface states rather than the bulk, and determine $\mathbf{J}^{\mathrm{NL}}$ for these states without making a multipole expansion. The model of a homogeneous solid with an abrupt change in the linear and nonlinear susceptibilities at the boundary yields, however, a surprisingly good description of the observed effects from bound electrons, when the effective averages $\bar{\beta}$ and $\bar{\delta}$ are taken about equal to one-half of their bulk values. The results (35) and (36) are equivalent to those obtained by Jha and Warke[16] if we take $\delta=\bar{\delta}=0$ and $\bar{\beta}=\beta$. For conduction electron plasma, $\bar{\beta}=\beta$, since it is constant in the thin layer at the surface. Our results are also the same as those obtained by Wang and Duminski[12] if we make the following substitutions, $P_{\perp}^{1/2}=E_{2\perp}{}^{R}(\phi=45°)A^{1/2}$, $P_{\parallel}{}^{1/2}=E_{2\parallel}{}^{R}(\phi=45°)A^{1/2}$, and $P_{\gamma}{}^{1/2}=E_{1\parallel}{}^{R}(\phi=90°)A^{1/2}$, and if their $\alpha\sin^2\theta$ is replaced by $\frac{1}{2}\bar{\delta}\epsilon(2\omega)[\epsilon^2(\omega)-1]$. Actually, their coefficient $\alpha_{\mathrm{WD}}+2\gamma$ corresponds to our $\bar{\delta}$, although they apparently assumed the normal component of the surface polarization to be proportional to α_{WD}. Also, the right-hand side of Eq. (3) in their paper should be multiplied by a factor of 2, and γ should be changed to $-\gamma$ in Eq. (4).

V. DISCUSSION AND COMPARISON WITH EXPERIMENTAL RESULTS

For semiconductors and insulators one expects, according to Eq. (17), that at low frequencies $\bar{\delta}=0$ and $\beta=-2\gamma\approx 2\bar{\beta}$. For materials with a high dielectric constant, it then follows that the dominant term in Eq. (35) is the term in $\bar{\beta}$, except when $\phi=90°$. The drawn curve in Fig. 5 describes the theoretical dependence of the square of this term on the angle of incidence, θ. The agreement with the experimental data is adequate and the behavior is largely determined by the function $\sin^2\theta\cos^4\theta$. This remains true even if $\delta\neq 0$. Therefore, the angular dependence in metals, where one has a contribution of the valence electrons according to Eq. (17) as well as a conduction-electron contribution according to Eq. (18), is also about the same as observed, if we use the experimental values for the linear dielectric constants. The dominant nonlinear surface terms are also responsible for the dependence of the harmonic intensity on ϕ. The last two terms in Eq. (35) predict a $\cos^4\phi$ dependence both for Ag and Si, as shown in Fig. 4.

For metals, the plasma contribution to the nonlinearity is usually larger than the nonlinear contribution arising from interband transitions of the valence electrons, which may still be estimated from Eq. (17), if one uses their contribution to the linear susceptibility for $\chi_{\mathrm{val}}{}^{\mathrm{L}}(\omega)$. The latter is quite important for Ag and Au and their alloys and should always be taken into account in the Fresnel factors. The magnitude and dispersion of the nonlinearity in these metals have been discussed by several authors.[8–10,15–17] In Table I we compare our experimental value for the ratio

$$M=|E^{R}_{2\parallel}(\theta=45°,\phi=90°)|^2|E^{R}_{2\parallel}(\theta=45°,\phi=0°)|^{-2}$$

with the theoretical values for M. The valence electron contribution to the linear dielectric constant is taken into account, but their nonlinear contribution is assumed to be zero in the next to last column of Table I. Rustagi's[17] estimate of this nonlinear interband contribution improves the agreement, as shown in the last column.

The low-frequency relations $\bar{\delta}=0$ and $\bar{\beta}=-\gamma$ should be most applicable to transparent materials. This relation predicts that the ratio $(P_{\perp}/P_{\parallel})^{1/2}=(E^{R}_{2\perp}/E^{R}_{2\parallel})$ is independent of the nonlinear coefficients, depending only on the linear dielectric constant and on angles θ and ϕ, and going to zero for both $\phi=0°$ and $\phi=90°$. Wang and Duminski[12] have tabulated this experimental ratio for several ionic crystals, with $\theta=60°$ and $\phi=45°$. Since the refractive indices of these compounds are close to 1.5, one finds this ratio from Eqs. (34) and (35) to be of the order 2 for all these compounds. The experimental values for $(P_{\perp}/P_{\parallel})^{1/2}$ are close to unity. The agreement with the theory may be improved by assuming that $\bar{\delta}\approx 0.5\beta$ owing to the existence of a surface layer. Wang and Duminski report for this ratio a higher experimental value $\bar{\delta}/\bar{\beta}=4$ for the alkali halides. If we use, however, the form given by Eq. (35), i.e., replace $\bar{\delta}\sin^2\theta$ by $\frac{1}{2}\bar{\delta}[\epsilon^2(\omega)-1]\epsilon(2\omega)$, the corresponding $\bar{\delta}$ values are reduced to $\bar{\delta}/\bar{\beta}\approx 0.6$. Furthermore, the detailed averaging over the surface layer would become more critical for relatively low-index materials. Therefore, the observations are not necessarily in contradiction with the fact that δ should vanish for the bulk of these ionic crystals. One should expect the signal from low-index materials to be more sensitive to the detailed structure of adsorbed molecular layers, although Wang and Duminski state that their results are independent of the surface treatment. At any rate, the observed angular and polarization dependence in these materials is not inconsistent.

One can understand why the results in the high dielectric-constant materials are essentially independent of the surface treatment and adsorbed layers, such as oxides or hydroxyl groups. The nonlinearity of the latter is much smaller than that of the first layer of the atomic bulk material. The harmonic signal was observed to be independent of the orientation of the surface cut with respect to the crystallographic axes in Si and Ge. This is in agreement with the form of Eq. (7), which is identical for cubic and isotropic materials.

Whereas the magnitude of our observations on Si and Ge agree with those reported by Wang and Duminski, there is a discrepancy in the SH intensity, polarized perpendicular to the plane of incidence. We were unable to detect this intensity. With the assumption $\beta=-2\gamma$ and $\delta=0$, we find from Eqs. (34) and (35) for the ratio

$$|E^{R}_{2\perp}(\theta=45°,\phi=45°)|^2|E^{R}_{2\parallel}(\theta=45°,\phi=45°)|^{-2}=0.01,$$

and the perpendicular polarization of the harmonic

TABLE III. Comparison between theoretical and experimental values of the quadrupolar nonlinear coefficient.

	Density of valence electrons, $(10^{23}\ \mathrm{cm}^{-3})\mathfrak{N}$	Harmonic photon energy (eV)	$\bar{\beta}(10^{-16}$ esu) expt.	$\frac{1}{2}\beta(10^{-16}$ esu) from Eq. (17)
Si	2.0	2.87	48[a]	30
Ge	1.8	2.87	80[a]	62
CaF_2	1.5	3.58	0.4[b]	0.35
BaF_2	1.0	3.58	0.4[b]	0.40
KCl	0.96	3.58	0.6[b]	0.75
NaCl	1.3	3.58	0.55[b]	0.65
LiF	3.2	3.58	0.5[b]	0.15
NaF	2.4	3.58	0.5[b]	0.20
MgO	3.2	3.58	1.2[b]	0.70
KBr	0.85	3.58	0.45[b]	1.0
KI	0.65	3.58	0.55[b]	2.5
$CaCO_3$	1.00	3.92	1.1[c]	0.75

[a] This work.
[b] From Ref. 12.
[c] From Ref. 21. This is a bulk effect in a noncubic crystal, and $\bar{\beta}$ should be identified with β. See text for further details.

would indeed fall just below our detection limit. Wang and Duminski list $\gamma/\beta=10$ for Si and $\gamma/\beta=17$ for Ge. If these higher values were correct, they would present a serious difficulty for our low-frequency theory.

We now turn to the magnitude of the nonlinear coefficients. The experimental value for β may be determined from the data listed in Table II for Si and Ge. For comparison with the theory, we take our data at the lower frequencies. We list these in Table III together with the data of Wang and Duminski for several ionic crystals of cubic symmetry. We compare these with values of $\frac{1}{2}\beta$, calculated from Eq. (17) with the known index of refraction and density of valence electrons.

The agreement between our simple theory and experiment seems to be quite good, except for KBr and KI. We have consistently assumed the P band to be the valence band for all the ionic crystals. However, for KBr $3d$ and $4s$ bands, and for KI $4d$ and $5s$ bands overlap with their P bands. The effective density of electrons in valence bands is therefore expected to be much higher in these solids, which will reduce the calculated values of $\frac{1}{2}\beta$ accordingly.

Bjorkholm and Siegman[21] have measured the quadrupole nonlinearity in calcite very accurately. This value is determined from the bulk effect, with a helium-neon laser beam in a phase-matched condition. Unlike in cubic crystals, the volume term may drive the SH wave in anisotropic crystals, if either the fundamental or harmonic is an extraordinary wave. Calcite has $\bar{3}m$ symmetry and the observed nonlinearity is a linear combination of the coefficients $N\Gamma_{xxzz}$ and $N\Gamma_{xxyy}$ in Eq. (5). In order to make the comparison with cubic crystals, we have assumed[21] $N\Gamma_{xxzz}\approx N\Gamma_{xxyy}=\beta$ for the entry in Table III. Again the order of magnitude is well confirmed by the theoretical model.

It may be concluded that the SHG in reflection from media with inversion symmetry is described rather well by the quadrupole-type nonlinear properties calculated for the homogeneous bulk material with an abrupt discontinuity at the boundary. The order of magnitude can be correctly related to the linear dielectric constant in insulators. There is a marked trend of increasing nonlinearity with increasing dielectric constant. The bound electrons also contribute significantly to the nonlinearity in metals.

The directional and polarization properties are well described by a combination of linear and nonlinear Fresnel factors. In materials with a high dielectric constant, the dominant contribution comes from the first layer of atoms in the bulk material. Adsorbed molecular layers have relatively little effect, because they have a much smaller dielectric constant and hence a much smaller nonlinearity. The angular dependence in alkali halides and other ionic crystals with rather lower dielectric constant is more complex as the contributions of the various terms in Eqs. (34) and (35) become more nearly equal to one another.

In principle, the accurate determination of the quadrupole-type nonlinearity could also give information about the electronic structure at the surface. At present, the experimental data do not permit us to draw any detailed conclusions about such a structure. The magnitude of the weak harmonic signals is consistent with a model in which the linear and nonlinear susceptibilities of the homogeneous bulk material drop abruptly to zero at the boundary. It is remarkable that the optical quadrupole-type terms, which escape experimental detection at the fundamental frequency, should be observable in SHG because of the excellent discrimination between the light frequencies. It is essentially a "null method."

ACKNOWLEDGMENTS

We would like to thank Professor P. S. Pershan for discussions on the relationship between the volume quadrupole and the surface dipole effects. Helpful discussions with Professor H. Ehrenreich on the optical properties of metals are also acknowledged. We also wish to thank Mr. S. Maurici for his assistance in crystal polishing.

[21] J. E. Bjorkholm and A. E. Siegman, Phys. Rev. **154**, 851 (1967). Their coefficient η_{13} corresponds to $\frac{1}{2}N\Gamma_{xxzz}$ in our notation, etc.